arXiv:astro-ph/9812178v1 9 Dec 1998

Interferometric Observations of Redshifted Molecular Absorption toward Gravitational Lenses

Karl M. Menten

Max-Planck-Institut für Radioastronomie, Auf dem Hügel 69, D-53121 Bonn, Germany (kmenten@mpifr-bonn.mpg.de)

Christopher L. Carilli

National Radio Astronomy Observatory, P.O. Box 0, Socorro, NM 87801, USA (ccarilli@aoc.nrao.edu)

Mark J. Reid

Harvard-Smithsonian Center for Astrophysics, 60 Garden Street, Cambridge, MA 02138, USA (reid@cfa.harvard.edu)

Abstract.

We have made radio- and millimeter-wavelength interferometric observations of a variety of molecular absorption lines toward the gravitational lens systems B0218+357 and PKS 1830−211. The absorption occurs in the lensing galaxies at redshifts of 0.685 and 0.89, respectively. The high spatial resolution of our VLA and VLBA observations allows imaging of the background continuum emission and the absorption distribution. Our multi-transition studies yield estimates of the cosmic microwave background temperature at $z = 0.89$ and determinations of molecular and isotopic abundance ratios, which allow meaningful comparisons with Galactic molecular clouds.

1. Introduction

The discovery by Wiklind & Combes of high-redshift molecular absorption toward four radio sources provides a novel approach of studying the dense interstellar medium of galaxies at cosmological distances. In two of the detected sources, 1504+377 and 1413+135, the absorption takes place in the host galaxy of the active galactic nucleus (AGN) providing the background continuum emission (Wiklind & Combes 1994, 1996a). In the other two systems, B0218+357 and PKS 1830−211, the absorption occurs in galaxies that act as gravitational lenses magnifying the radio- and millimeter-wavelength emission of a background AGN. In both of the latter sources the absorbing material, which is, respectively, at redshifts near 0.685 and 0.89, has a remarkably high molecular hydrogen column density exceeding 10^{22} cm^{-2} (Wiklind & Combes 1995, 1996b; Menten & Reid 1996). Particularly toward PKS 1830−211, one observes a wide variety of absorption lines from a series of high dipole moment species that are well-known constituents of molecular clouds within the Milky Way (Wiklind &

Combes 1996b, 1998). Here we report interferometric observations targeted at understanding the spatial distribution and chemical composition of the absorbing clouds observed toward B0218+357 and PKS 1830−211.

2. Observations

We have used the VLA to search for absorption from a number of molecules toward B0218+357 and PKS 1830−211. In particular, the $J = 1 - 0$ rotational ground state lines from the high dipole moment species HCO^+, HCN, and HNC, which are detected toward many Milky Way molecular clouds, have rest frequencies in the 3 mm band that are redshifted into the 38–49 GHz range covered by the VLA's "new" highest frequency receivers for $z \approx 0.83$ – 1.3. At the time of our observations, 13 VLA antennas were equipped with 38–49 GHz receivers. Toward PKS 1830−211, we detected absorption from the $J = 1 - 0$ lines of the three molecules mentioned, as well as from the analogous transitions of their ^{13}C-substituted isotopomers. In addition, we detected absorption from the C_3H_2, HC_3N, H_2CO, and C_2H molecules. Our VLA observations allow for accurate optical depth determinations. Moreover, since some of our observations used the highest resolution A configuration, we are able to image the PKS 1830−211 system at $0\farcs1$ resolution. The observations described here are part of an extensive program of studying molecular absorption toward PKS 1830−211 and B0218+357 that also includes observations with the IRAM interferometer, the Effelsberg 100 m telescope, and the Very Long Baseline Array (VLBA).

3. PKS 1830−211: Morphology and Spatial Extent of the Absorption

The upper left panel of Fig. 1 shows a 47.0 GHz VLA map of the PKS 1830−211 gravitational lens system made with a resolution of $0\farcs1$. Two compact sources, in the following referred to as the NE and SW images, with weak extended "tails" are seen, displaying the inversion symmetry expected from gravitational lensing of a core/jet source. With decreasing frequency, the jet components grow larger (Rao & Subrahmanyan 1988; Subrahmanyan et al. 1990) and form an Einstein ring (Jauncey et al. 1991), which is *not* resolved in our $0\farcs75$ resolution 7.7 GHz map shown in the lower left panel of Fig. 1.

Also shown in Fig. 1 are spectra of the HCN $J = 1 - 0$ line made toward both images. Strong absorption with a peak optical depth $\gtrsim 2$ is observed at zero velocity (assuming $z = 0.88582$) toward the compact core of the SW image, while much weaker absorption is observed in the same transition toward the NE image at a 147 km s^{-1} lower velocity. This general distribution of the HCN absorption is consistent with the results obtained for the $2 - 1$ line of this molecule by Frye, Welch, & Broadhurst (1997) and Wiklind & Combes (1998). Our higher resolution VLA observations, together with VLBA data on the HC_3N $J = 5 - 4$ line (redshifted to 24.1 GHz; Carilli et al. 1998) allow for a more detailed analysis of the spatial structure of the molecular absorption toward PKS 1830−211(SW). As discussed by Carilli et al. (1998), the HC_3N absorption is arising from a region of size larger than 2.5 milliarcseconds or $10h^{-1}$ pc, where h is the Hubble constant in units of 100 km s^{-1} Mpc^{-1} and

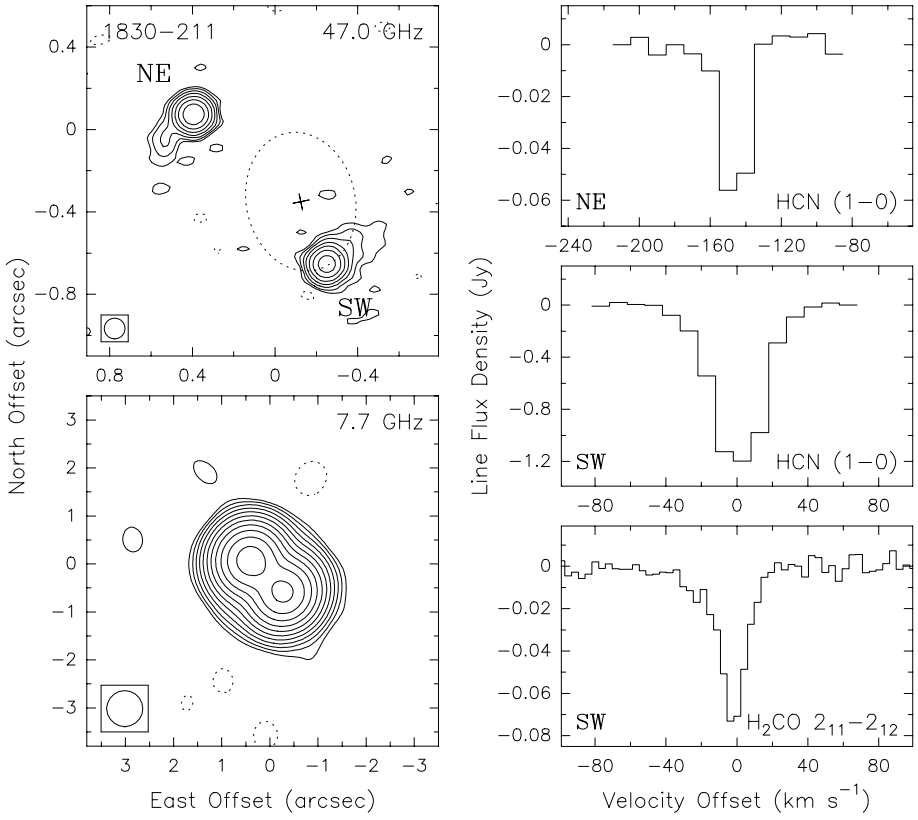

Figure 1. VLA continuum images and molecular absorption spectra of PKS 1830−211. The upper and lower left panels show continuum maps made with the VLA at frequencies of 47 and 7.7 GHz, respectively. Note that the 7.7 GHz map shows a larger field. The 47 and 7.7 GHz maps were restored with circular beams, indicated in the lower left map corners, of size 0.″1 and 0.″75 (FWHM), respectively. The cross and dotted ellipse in the 47 GHz map indicate the centroid position, orientation, and core size of the oblate spheroidal lens mass distribution assumed in the lens model of Nair et al. 1993, which has a core radius of 0.″34 and an eccentricity of 0.63. The upper two panels on the right hand side show absorption spectra of the HCN $1-0$ rotational transition taken toward the north-eastern (NE) and south-western (SW) images, respectively, while the lower right panel shows a spectrum of the $2_{11}-2_{12}$ line of H_2CO toward the SW image. The velocity scales of all spectra are in the heliocentric system with zero velocity corresponding to $z = 0.88582$.

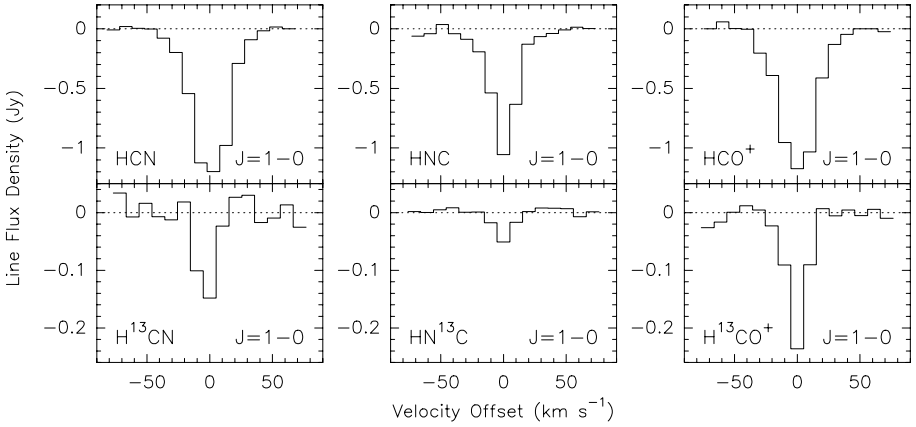

Figure 2. Spectra of the redshifted $J = 1 - 0$ transition from the main isotopomers of HCN, HNC, and HCO^+ observed toward PKS 1830−211 (SW) are shown in the upper row, while spectra of the same transition from the ^{13}C substituted isotopomers are shown in the lower row. The velocity scales of all spectra are in the heliocentric system with zero velocity corresponding to $z = 0.88582$.

$q_0 = 0.5$ is assumed. An upper limit of $\sim 600h^{-1}$ pc on the size of the absorbing cloud follows from the fact that we do not detect HCN absorption toward the tail of SW image with an upper limit on the optical depth of 0.3.

As discussed by Wiklind & Combes (1998), the observed difference in absorption velocities between the SW and NE images allows for tight constraints on the lens mass distribution and, thus, lensing models of PKS 1830−211 (see Kochanek & Narayan 1992; Nair, Narasimha, & Rao 1993). Wiklind & Combes (1998) derive $V_0 \approx 220\sqrt{D}$ km s^{-1} for the rotation velocity, V_0, of the $z \approx 0.89$ lensing galaxy. The "effective distance" D, measured in Gpc, is equal to $D_l D_s / D_{ls}$; where D_l is the distance between the observer and the lens, D_s the distance between the observer and the source, and D_{ls} the distance between the lens and the source. All distances are angular diameter distances. Very recently, a value of 2.507 has been measured for the redshift of the lensed source in the PKS 1830−211 system (see the report by Lidman 1998), yielding $V_0 \approx 366$ km s^{-1} and an inclination angle, i, of 16° ($H_0 = 75$ km s^{-1} Mpc^{-1} and $q_0 = 0.5$ are assumed throughout this paper). This indicates that the lensing galaxy is a massive early-type spiral. There is, however, the possible complication of multiple lensing, which might be expected, given the presence of an HI absorption system at a redshift of 0.1927 (Lovell et al. 1996).

4. Astrochemistry at $z = 0.88582$

4.1. Gas Excitation and Temperature of the Cosmic Microwave Background

Figs. 1, 2, and 3 show examples of absorption line spectra toward the PKS 1830−211 (SW) source resulting from our VLA observations. For some species

Table 1. Molecules toward PKS1830−211 and Galactic Clouds

Species	μ (D)	N(PKS 1830−211) (cm^{-2})	$N(X)/N(CO)\times10^6$ ..... PKS 1830−211	TMC-1	L 183	3C111	NRAO 150
CO	0.11	3.0×10^{18}	1	1	1	1	1
CS	1.96	4.8×10^{14}	160	130	9		
HCO^+	3.30	4.0×10^{14}	130	110	100	130	180–1400
HCN	2.98	3.2×10^{14}	110	130	40		400–2000
HNC	2.70	1.2×10^{14}	40	250	<50		
N_2H^+	3.40	5.4×10^{13}	18	10	∼10		
CCH	0.8	7.9×10^{14}	260	>100	<100		
H_2CO	2.33	3.8×10^{14}	130	250	250	220	590–1200
C_3H_2	3.4	6.7×10^{12}	2	130	3	56	190
HC_3N	3.72	8.1×10^{12}	3	75	1		
OH	1.67	4.1×10^{15}	1400	3800	940	250	

The first, second, and third columns list, respectively, molecular species detected toward PKS 1830−211, their dipole moments (in Debyes), and column densities in the $z = 0.88582$ absorbing cloud measured toward PKS 1830−211(SW). Column densities of species listed in italics are *not* derived from our data but are taken from Wiklind & Combes 1996b and, for CO and OH, from Gerin et al. 1997 and Chengalur, de Bruyn, & Narasimha (this volume), respectively. The remaining columns list for PKS 1830−211 and four well-studied Galactic molecular clouds the column densities measured for the various species multiplied by 10^6 and divided by the column density of CO in the clouds in question. The Galactic clouds considered are the dark clouds TMC-1 and L 183 (also known as L 134 N; see Irvine et al. 1987 and van Dishoeck et al. 1993 and references therein for abundances) and the diffuse clouds seen in absorption against the extragalactic radio sources 3C111 and NRAO 150 (Liszt & Lucas 1995, 1998; Lucas & Liszt 1996; and Cox, Güsten, & Henkel 1988). For NRAO 150 the range of values observed for the various absorption components occurring at different radial velocities is given, except for the case of C_3H_2.

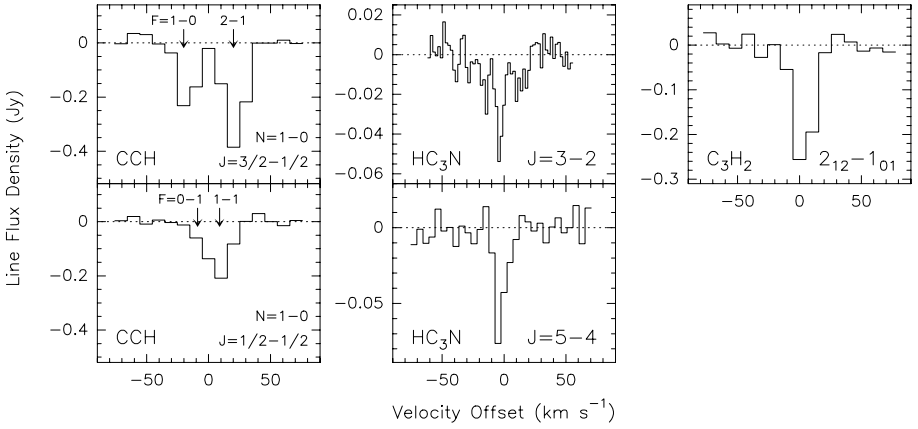

Figure 3. Redshifted absorption spectra of various hyperfine components of the $N = 1-0$ transition of CCH (left hand panels), the HC_3N $J = 3-2$ and $5-4$ transitions (middle panels), and the $2_{12} - 1_{01}$ transition of C_3H_2 (right hand panel) observed with the VLA toward PKS 1830−211. The velocity scales of all spectra are in the heliocentric system with zero velocity corresponding to $z = 0.88582$.

we can compare our measured optical depths with the values determined by Wiklind & Combes (1996b) for higher excitation lines of the same species. We find that to within the uncertainties of a few K, the thus determined rotation temperatures, $T_{\rm rot}$, are consistent with the value of the cosmic microwave background temperature, $T_{\rm cmb}$, at $z = 0.89$. All of the species observed by us have high dipole moments (see Table 1). Even for the relatively low frequency HC_3N lines, the critical densities necessary for thermalization of the level populations at or near the kinetic temperature, $T_{\rm kin}$, are $\gtrsim 10^4$ cm^{-3}. Therefore, the low rotation temperatures indicate subthermal excitation due to a relatively low total density of the absorbing cloud rather than low kinetic temperatures, which for molecular clouds within the Milky Way are generally greater than 10 K.

Given that $T_{\rm rot} = T_{\rm cmb}$, the accurate optical depth determinations afforded by our interferometer measurements allow for a meaningful estimate of the cosmic microwave background temperature at $z = 0.89$, for which big bang theory predicts a value of $(1+z)$ 2.73 K = 5.14 K. In particular, from the HC_3N $J = 3-2$ and $5-4$ spectra shown in Fig. 3 we derive $T_{\rm rot} = 4.5^{+1.5}_{-0.6}$ K. We note that the errors quoted for the HC_3N rotation temperature are formal uncertainties and do not take into consideration systematic effects such as variations in the source covering factor between 14.5 and 24.1 GHz, the frequencies of the redshifted $3-2$ and $5-4$ lines.

4.2. Molecular Abundances – Comparison with Galactic Clouds

From our measured optical depths we calculate the total column densities for HCO^+, HCN, HNC, CCH, H_2CO, C_3H_2, and HC_3N listed in Table 1, assuming that the level populations are thermalized at $T_{\rm cmb} = 5.14$ K. Table 1 also shows a comparison of the abundances of molecules detected toward PKS 1830−211 with the values measured toward four Galactic molecular clouds. Listed are the

abundances of the various species (multiplied by 10^6) relative to the CO column density. The Galactic clouds in question are the cold, dense dark clouds TMC-1 and L 183 and the more diffuse clouds seen against the extragalactic radio sources 3C111 and NRAO 150. The dark clouds have CO column densities, N(CO), of order a few times 10^{18} cm^{-2} and [CO/H_2] abundance ratios $\approx 8 \times 10^{-5}$ (Irvine et al. 1985; van Dishoeck et al. 1993 and references therein); while Liszt & Lucas (1998) determine $N(\mathrm{CO}) = 9 \times 10^{16}$ cm^{-2} for 3C111 and N(CO) values in the range $(0.25 - 6.6) \times 10^{15}$ cm^{-2} for the various radial velocity components of the multiple-cloud absorption system observed toward NRAO 150. The 3C111 absorber and most of the absorbing clouds seen toward NRAO 150 are quite dense compared to "typical" diffuse clouds studied, e.g., by ultraviolet absorption spectroscopy and probably have [CO/H_2] abundance ratios exceeding 10^{-5}. By comparison, for the diffuse cloud sample discussed by Federman et al. (1994; see also Liszt & Lucas 1998) [CO/H_2] abundance ratios range from a few times 10^{-8} to a few times 10^{-6}.

It is clear from Table 1 that the PKS 1830−211 absorbing cloud has a total column density and molecular abundances that are quite similar to the values found in Galactic dark clouds (note that C_3H_2 and HC_3N are anomalously overabundant in TMC-1 by Galactic molecular cloud standards). The $z = 0.88582$ cloud does not show the surprisingly high abundances of HCO^+, HCN, and H_2CO relative to CO found in the more diffuse Galactic clouds seen in absorption toward 3C111 and NRAO 150 and other sources, which are, particularly in the case of H_2CO, a challenge to current models of diffuse cloud chemistry (Turner 1994; Liszt & Lucas 1995).

While there are chemical similarities, a comparison of cloud structure in space and velocity reveals remarkable differences between the $z = 0.88582$ absorbing cloud and typical Galactic dark clouds such as TMC-1 or L 183. Assume that for the PKS 1830−211 (SW) cloud the abundance ratios of, say, the widespread CO, HCO^+, and HCN molecules relative to H_2 are similar to the values found for Galactic dark clouds. This implies a total molecular hydrogen column density of a few times 10^{22} cm^{-2}. Assuming further that the molecular hydrogen density is smaller than 10^4 cm^{-3}, as implied by the subthermal excitation of all of the high dipole moment species, we derive a pathlength larger than ~ 1 pc along the line of sight, which is to be compared with the 13 pc *lower* limit of the source size in the plane of the sky indicated by the VLBA results of Carilli et al. (1998) discussed above. To compare with Galactic molecular clouds, it is instructive to take as a reference source the nearby and well-studied Taurus/Auriga dark cloud complex (see, e.g., Cernicharo 1991), which has a total extent of ~ 50 pc, while individual clouds within that complex, such as TMC-1, have sizes of one to a few pc. The line widths in such clouds are < 1 km s^{-1}, and radial velocities are within ~ 1 km s^{-1} of a median value, with only a few km s^{-1} variation over the whole extent of the complex. In contrast, from, e.g., the high quality spectrum of the optically thin H_2CO absorption line (see Fig. 1), we find that the $z = 0.88582$ absorption covers a total velocity range of $\gtrsim 35$ km s^{-1} (FWZP), which is significantly larger than the velocity spread even of a Galactic giant molecular cloud (GMC), with the exception of the remarkable GMCs found within ~ 200 pc of the Galactic center. The latter clouds have velocity widths that are comparable to that of the $z = 0.88582$ absorber. We note that compared to the distance of these GMCs to the Galactic center, the cloud

absorbing PKS 1830−211 (SW) is located much further away from the center of the lensing galaxy, 1.8 kpc in the context of the model of Nair et al. (1993) and 3 kpc in the model by Kochanek & Narayan (1992). This possibly indicates significant differences in molecular cloud structure and composition between the $z = 0.88582$ lensing galaxy of PKS 1830−211 and the Milky Way.

4.3. Isotopic Abundance Ratios

Fig. 2 shows spectra of the redshifted $J = 1 - 0$ transitions of HCN, HNC, and HCO^+ together with spectra of the analogous transitions from the ^{13}C-substituted isotopomers. Of the three main isotopic lines, the HNC line has the lowest optical depth (≈ 1.2), affording, together with the optically thin $H^{13}CN$ line, a meaningful estimate of the $[^{12}C/^{13}C]$ ratio; we find a value of ≈ 35. The $[^{12}C/^{13}C]$ ratios determined from HCN and HCO^+ are consistent with this number. While the $[^{12}C/^{13}C]$ ratio in the $z = 0.88582$ cloud is smaller than the values found in the solar system and the local interstellar medium, $[^{12}C/^{13}C]$ ratios around 50 are measured for inner Galaxy clouds within 4 kpc of the Galactic center, while the Galactic center clouds themselves have even smaller values around 20 (see Wilson & Matteucci 1992; Wilson & Rood 1994).

^{13}C is only produced in low and intermediate mass stars, while ^{12}C is also produced in massive stars. Thus, the $[^{12}C/^{13}C]$ ratio is expected to decrease in time and with increasing stellar processing (see the discussion of Wilson & Matteucci 1992). The relatively low value measured at $z = 0.88582$ may thus be of interest in the context of chemical evolution studies. However, we note that we only sample one line of sight in the lensing galaxy, which might have an atypical chemical history.

We also searched unsuccessfully for absorption the DCN $(1 - 0)$ transition. Our upper limit and other searches for deuterated molecules toward PKS 1830−211 are discussed by Shah et al. (this volume).

5. A Multi-Transition Study of Formaldehyde at $z = 0.68466$ toward B0218+357

Formaldehyde (H_2CO) was first observed toward the Einstein ring B0218+357 in its 2 cm rest wavelength $2_{11} - 2_{12}$ K-doublet transition by Menten & Reid (1996), who found absorption toward the south-western of the two compact images of the background source, labeled A in Fig. 4 (see also Patnaik et al. 1993 and Patnaik & Porcas, this volume, for a description of the radio continuum morphology). The H_2CO absorption occurs at $z = 0.68466$, the same redshift at which Wiklind & Combes (1995) detect absorption from other molecules.

The populations of the $1_{10} - 1_{11}$ and $2_{11} - 2_{12}$ K-doublet transitions at 6 and 2 cm wavelength, respectively, are sensitively dependent on the H_2 density and these lines are usually anti-inverted. Statistical equilibrium calculations yield excitation temperatures and optical depths, so that comparisons with observations in principle allow meaningful estimates of the molecular hydrogen density (see, e.g., Henkel, Walmsley, & Wilson 1980). While both the 6 and the 2 cm transitions have now been detected toward B0218+357 (Fig. 4), their interpretation is complicated by the fact that the extent and intensity of the background continuum emission is strongly dependent on the observing frequency (see Patnaik

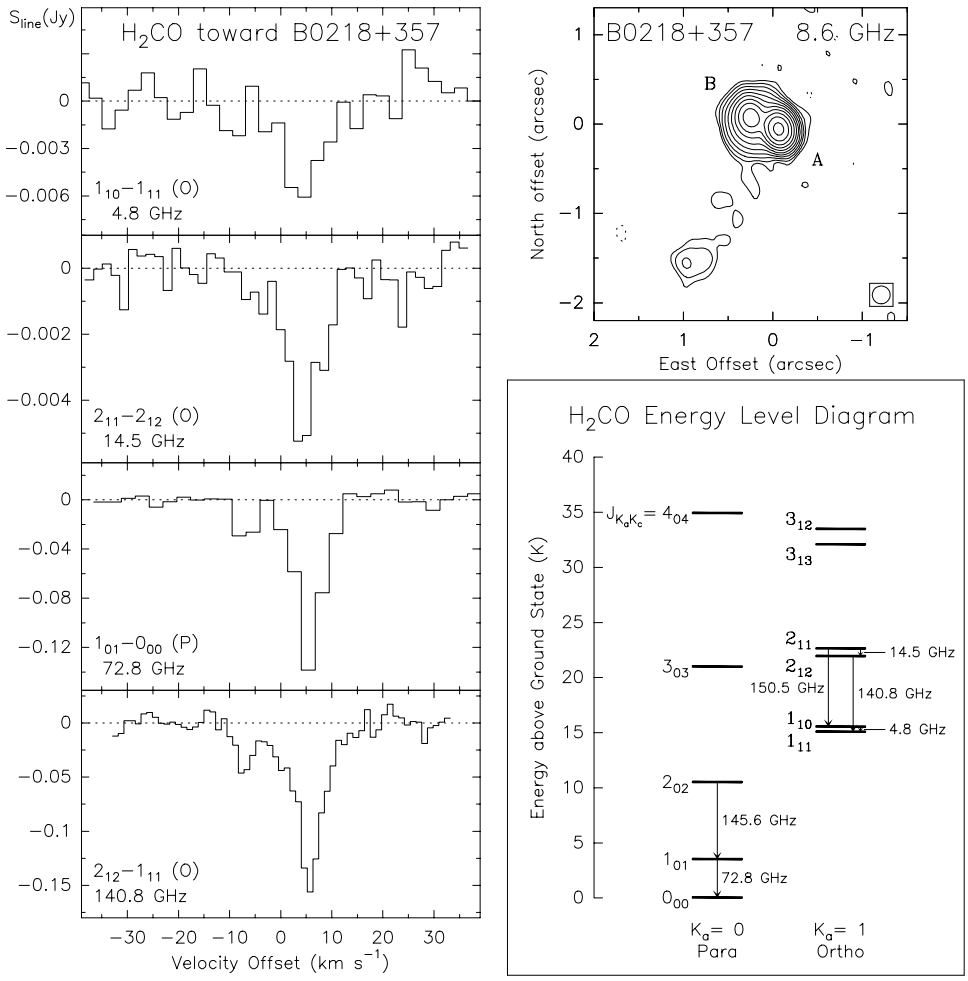

Figure 4. The left four panels show redshifted absorption spectra of several H_2CO transitions toward B0218+357. The top and bottom spectra were taken with the Effelsberg 100 m telescope and the IRAM interferometer, respectively, while the other two spectra were observed with the VLA. The labels in the left bottom corner of each spectrum list the transition and rest frequency. The O or P indicates whether the line in question is from ortho- or para-H_2CO. The velocity scales of all spectra are in the heliocentric system with zero velocity corresponding to $z = 0.68466$. The upper right panel shows a VLA continuum map of the B0218+357 gravitational lens system (from Menten & Reid 1996) made at 8.6 GHz, the frequency of the redshifted $2_{11} - 2_{12}$ transition. The H_2CO absorption occurs to the southwestern compact source A. The lower right panel shows an excerpt of the H_2CO rotational energy level diagram. Transitions that we measured toward B0218+357 are shown as arrows, with rest frequencies indicated.

& Porcas, this volume). Modeling of the H_2CO excitation will be greatly aided by VLBI observations and determinations of the excitation temperatures of the 6 cm and 2 cm lines, which can be extracted from observations of millimeter-wavelength lines interconnecting the energy levels of the centimeter lines (see Fig. 4). For this reason, we have also observed a number of millimeter-wavelength H_2CO transitions toward H_2CO. While spectra for several lines are shown in Fig. 4, the results of our model calculations will be presented in a future publication.

Since we have observed both ortho- and para-H_2CO lines, our observations allow an estimate of the ortho-to-para ratio, which should be 3 if the H_2CO was formed in warm gas ($T_{\rm kin} \gg 15$ K) or on hot dust grain surfaces and ≈ 1 for formation in cold gas or on cold grain surfaces.

From a preliminary analysis of the $1_{01} - 0_{00}$ para- and the $2_{12} - 1_{11}$ ortho-transition (see Fig. 4), we derive an ortho-to-para H_2CO ratio of 3.1 ± 0.2. Systematic uncertainties of this value are likely to be small, since, contrary to the case of the low frequency K-doublet transitions mentioned above, the covering factors of the two millimeter-wavelength transitions used in its derivation should be very similar.

Acknowledgments. The National Radio Astronomy Observatory is a facility of the National Science Foundation operated under cooperative agreement by Associated Universities, Inc.

References

Carilli, C. L., Menten, K. M., Reid, M. J., Rupen, M. P., & Claussen, M. 1998, in IAU Colloq. 164: Radio Emission from Galactic and Extragalactic Compact Sources, ed. J. A. Zensus, G. B. Taylor, & J. M. Wrobel (San Francisco: ASP), 317

Cernicharo, J. 1991, in The Physics of Star Formation and Early Stellar Evolution, ed. C. J. Lada & N. D. Kylafis (Dordrecht: Kluwer), 287

Cox, P., Güsten, R, & Henkel, C. 1988, A&A, 206, 108

Federman, S. R., Strom, C. J., Lambert, D. L., Cardelli, J. A., Smith, V. V., Joseph, C. L. 1994, ApJ, 424, 772

Frye, B., Welch, W. J., & Broadhurst, T. 1997, ApJ, 478, L25

Gerin, M., Phillips, T. G., Benford, D. J., Young, K. H., Menten, K. M., & Frye, B. 1997, ApJ, 488, L31

Henkel, C., Walmsley, C. M., & Wilson, T. L. 1980, A&A, 82, 41

Irvine, W. M., Schloerb, F. P., Hjalmarson, Å., & Herbst, E., 1985, in Protostars and Planets II, ed. D. C. Black & M. S. Matthews (Tucson: Univ. Arizona Press), 579

Jauncey, D. L., et al. 1991, Nature, 352, 132

Kochanek, C. S., & Narayan, R. 1992, 401, 461

Lidman, C. 1998, ESO Messenger, 93, 16

Liszt, H. , & Lucas, 1995, A&A, 299, 847

Liszt, H. S., & Lucas, 1998, A&A, 339, 561

Lucas, R., & Liszt, H. 1996, A&A, 307, 237

Lovell, J. E. J., et al. 1996, ApJ, 472, L5

Menten, K. M., & Reid, M. J. 1996, ApJ, 465, L99

Nair, S., Narasimha, D., & Rao, A. P. 1993, ApJ, 407, 46

Patnaik, A. R., Browne, I. W. A., King, L. J., Muxlow, T. W. B., Walsh, D., & Wilkinson, P. N. 1993, MNRAS, 261, 435

Rao, A. P., & Subrahmanyan, R. 1988, MNRAS, 231, 229

Subrahmanyan, R., Narasimha, D., Rao, A. P., & Swarup, G. 1990, MNRAS, 246, 263

Turner, B. E. 1994, ApJ, 437, 658

van Dishoeck, E. F., Blake, G. A., Draine, B. T., & Lunine, J. I. 1993, in Protostars & Planets III, ed. E. Levy & J. I. Lunine (Tucson: Univ. Arizona Press), 163

Wiklind, T., & Combes, F. 1994, A&A, 286, L9

Wiklind, T., & Combes, F. 1995, A&A, 299, 382

Wiklind, T., & Combes, F. 1996a, A&A, 315, 86

Wiklind, T., & Combes, F. 1996b, Nature, 379, 139

Wiklind, T., & Combes, F. 1998, ApJ, 500, 129

Wilson, T. L., & Rood, R. T. 1994, ARAA, 32, 191

Wilson, T. L., & Matteucci, F. 1992, A&AR, 4, 1